DIRECTIVITY ANALYSIS OF ANGLE PROBES AND SURFACE DEFECTS BY ULTRASONIC VISUALIZATION METHOD

Y.H. Nam and K. Date
Faculty of Engineering
Tohoku University
Sendai, Miyagi, 980-77 Japan

INTRODUCTION

An ultrasonic non-destructive testing uses the directivity of the ultrasonic wave which propagates in one direction. The directivity is expressed as the relationship between the propagate direction and its sound pressure. It is, therefore, important for an ultrasonic testing to know the ultrasonic directivity, because it is closely related to determination of probe arrangement, testing sensitivity and scanning pitch, and accuracy of defect location and characterization.

Since the sound pressure field in the solid cannot be measured directly, most of the study on ultrasonic directivity has been carried out in the theoretical field assuming the continuous wave.[1-5] However, the ultrasonic testing uses a pulse of elastic wave in a solid.

This paper studied the directivity of the elastic wave pulse from the direct observation of visualized wave. We examined the directivity of shear waves emitted from angle probes and scattered from artificial defects by applying ultrasonic visualization method. These experimental results were compared with the theory which was based on the continuous wave. The applicability of continuous wave theory was discussed in terms of the parameter d/λ; where d is transducer or defect size and λ is the wavelength.

VISUALIZATION SYSTEM

The configuration of the ultrasonic visualization system used in this study are diagrammed in Fig.1. The sound pressure images of visualized ultrasonic waves were obtained by synthesized photoelastic method[6] in the image-processing computer.

Review of Progress in Quantitative Nondestructive Evaluation, Vol. 14
Edited by D.O. Thompson and D.E. Chimenti, Plenum Press, New York, 1995

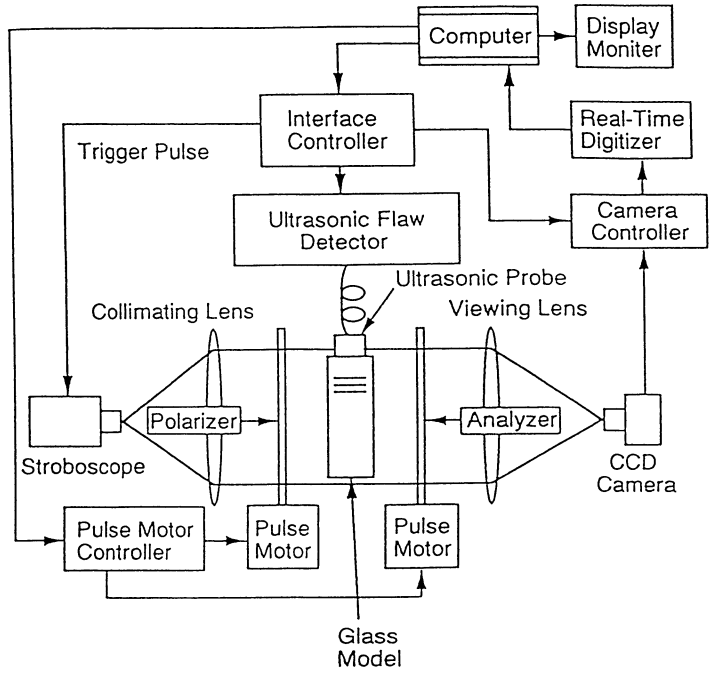

Fig.1 Diagram of sound pressure visualization system.

DIRECTIVITY ANALYSIS

Figures 2 illustrate the way of directivity determination from the visualized sound pressure images schematically.[7] We first determined the center point of directivity from the circular curvature of the visualized shear wave. Next, we set two circles, which have radius of r_1 and r_2, from the center to fix the examination range of sound pressure in θ direction. This is specially important for the directivity analysis of reflected shear wave from the defect, because ultrasonic scattering from the defect produces many reflected waves and it needs to discriminate the wave to be analyzed. The directivities of the wave were obtained from the relationship between the angle θ and the maximum sound pressure value on the line from r_1 to r_2.

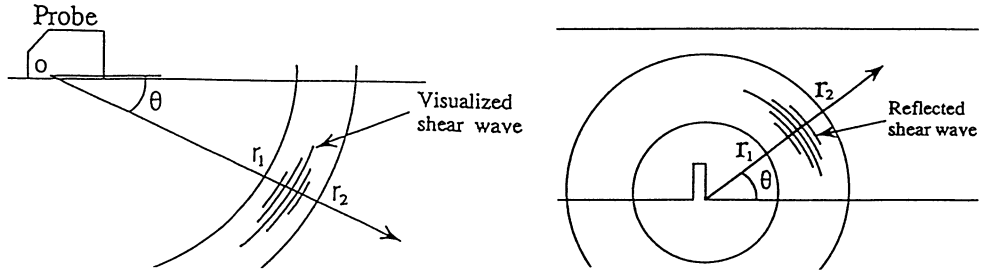

(a) Angle probe. (b) Surface defect.

Figs.2 Determination of directivity.

EXPERIMENTAL METHOD

Four types of angle probes were examined. Transducer size was all same; 8X9mm and the frequency were 2 and 4MHz, having nominal refraction angle of 45 and 60 degrees for steel.

Two types of rectangular specimen made of Pyrex glass were used for ultrasonic visualization experiments. The thickness of the specimens were 20mm. One has 300X50mm dimension for angle probe directivity examination. The other type is 145X15mm with artificial slit, whose width is 0.3mm, for defect directivity analysis. This type of specimens had various slit depth from 0.25 to 4mm.

The propagation distance of the emitted shear wave from the probe was fixed to 90mm in probe directivity measurement. In the case of defect directivity examination, we set the reflected shear wave after 10mm propagation from the slit root. The probe was put to the maximum echo height position from the slit.

Coupling agent used was machine oil.

COMPARED THEORY

Figure 3 shows the theoretical model of angle probe directivity analysis devised by K.Kimura.[8] The probe directivity $D_p(\theta)$ is expressed as follows;

$$D_p(\theta)=\sin E/E\cdot\cos\beta\cdot\cos\theta/\cos\alpha\cdot t(\theta) \qquad (1)$$

where $E=K_{1L}\cdot d\cdot\sin\beta$, $K_{1L}=2\pi/\lambda_{1L}$. In equation (1), sinE/E means the directivity of longitudinal wave in the wedge, in which the transducer shape is square of 2d, and the $t(\theta)$ is the transmission coefficient of

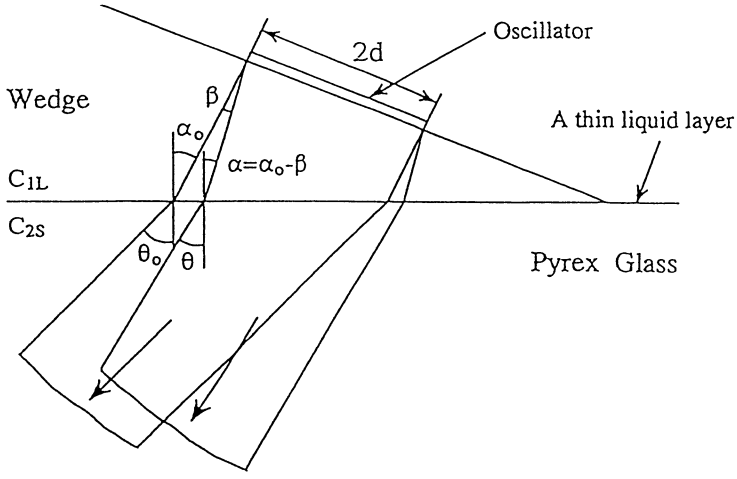

Fig.3 Model for angle probe directivity by K.Kimura.

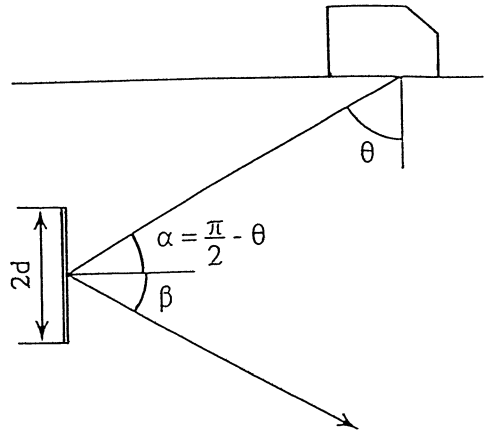

Fig. 4 Model of internal crack-like defect.

sound pressure from Acrylic wedge to Pyrex glass. λ_{1L} is the wavelength of longitudinal wave in wedge material.

We used the internal crack-like defect analysis [3][5] to compare with the experiment as shown in Fig. 4. Reflected wave directivity $D_F(\alpha, \beta)$ is;

$$D_F(\alpha, \beta)=2d\cdot\cos\alpha\cdot\sin X_t/X_t \qquad (2)$$

where $X_t=2\pi d/\lambda\cdot(\sin\beta-\sin\alpha)$ and λ is the wavelength.

In order to compare the internal crack like defect with surface slit, surface slit depth was taken to the half internal defect size d in Fig. 4. Validity of this correspondence was obtained in the perfect reflection of the shear wave at the bottom surface in the slit. This reflection occurred, when we used the angle probe of 45 degrees. In the case of 60 angle probe, bottom reflection produces the mode-conversion. So, we compared the directivity results obtained using angle probe of 45 degrees with the theoretical one, in which we set α=45 in equation (2).

RESULTS AND DISCUSSION

Directivity of Angle Probe

Figures 5 compare the measured directivity of angle probes with the theory. Principal lobe of the directivity agreed very well; however side lobes are not observed in the experimental results.

Directivity of Reflected Wave from Defect

Figures 6 shows the change of directivity with the slit depth and compared with the theoretical one. Note that there is sharp directivity in the case of small slit depth; d=0.25mm and 0.5mm, whereas weak

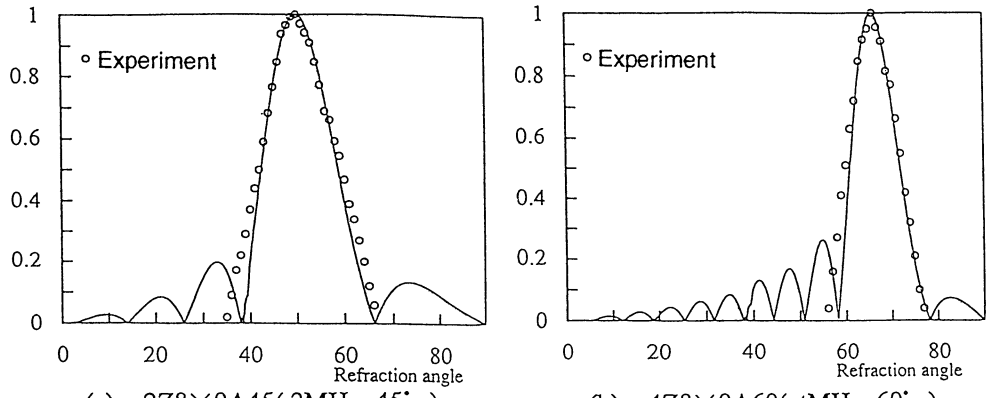

Fig. 5 Comparison of experimental directivity with theory in angle probes.

directivity was predicted in the continuous theory. The difference of the theory with the experiment is considered to be due to the effect of pulse, because the pulse contains the wide frequency component against the center frequency of the probe. In this case, the high frequency component of the pulse produces the sharp directivity as observed in the visualization experiments.

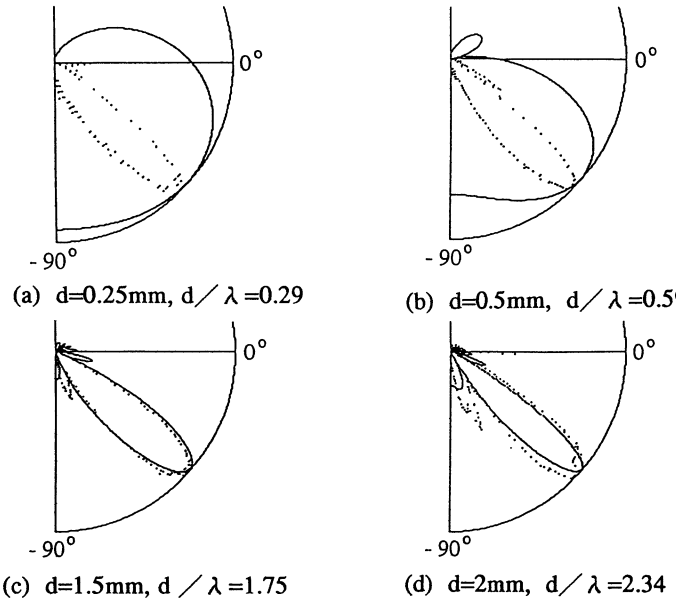

Figs. 6 Comparison of experimental directivity with theory for defects. Test frequency: 4MHz

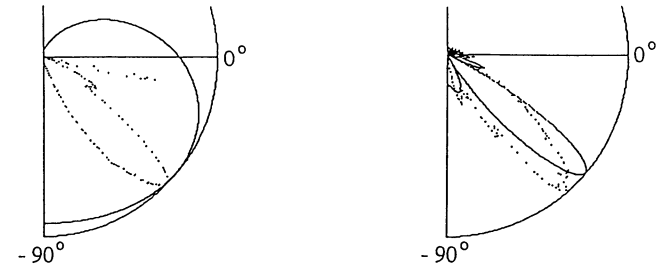

(a) d=0.5mm, d／λ=0.29 (b) d=4mm, d／λ=2.34

Figs.7 Comparison of directivity with parameter d/λ.
Test frequency:2MHz

In the case of large slit depth or large d/λ values as shown in Figs.6(c) and (d), the experiment and theory are well agreed. Figures 6 and 7 represent that the same directivities were obtained, when the parameter d/λ were the same.

Angle probes of 60 degrees produced complicated reflected waves from the slit as shown in Figs.8. Three peaks of the directivity were observed due to the mode conversion at the reflection of the slit. When d/λ value is the same, the similar directivity of single peak was also observed in 60° probes as shown in Figures 9.

Applicability of Continuous Wave Theory

The side lobe of the directivity is produced by the interference of continuous wave, for example, a first side lobe is due to the retardation of one wavelength. This interference is only possible for continuous wave, and the pulse wave having single peak doesn't produce the strong overlapping to make the side lobe. Figure 10(a) presents the single peak

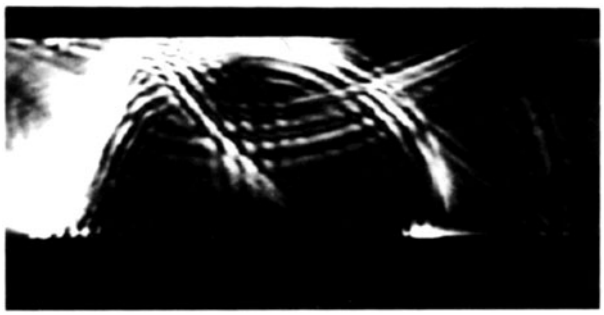

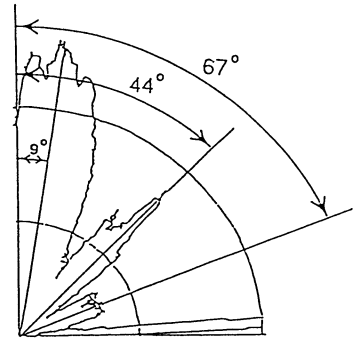

(a) Visualized shear waves scattered at defect (b) Directivity
Figs.8 Directivity of shear wave reflected from defect.(4MHz,60°,d=1mm)

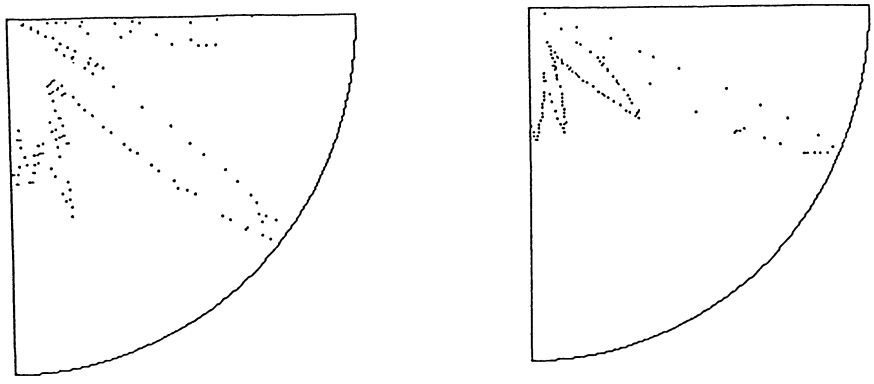

(a) d=0.75mm, 4MHz (b) d=1.5mm, 2MHz

Figs.9 Directivity of reflected shear wave (d/λ=0.88, 60° probe).

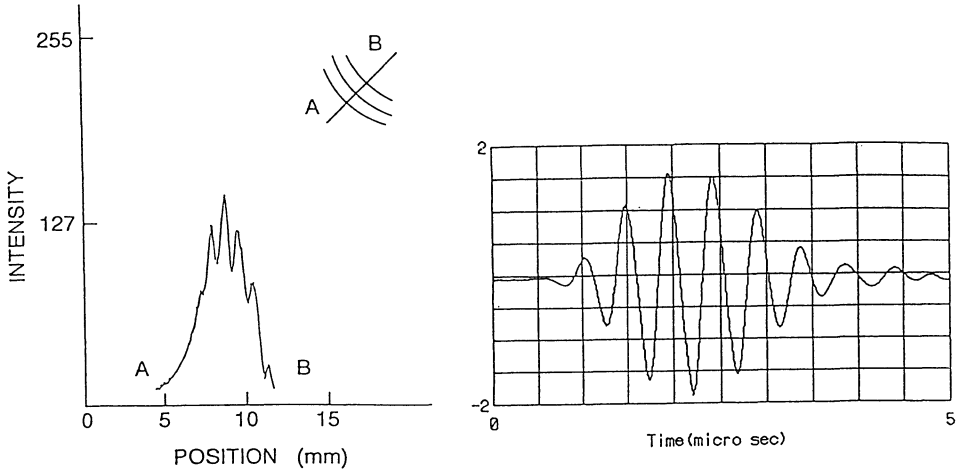

(a) Visualized waveform (absolute) (b) Echo signal waveform

Figs.10 Comparison of sound pressure waveform with echo signal waveform.

of absolute sound pressure waveform measured from the shear wave, which is emitted from the angle probe of 2MHz, 45°. That is, the sound pressure distribution from r_2 to r_1 in Fig.2(a). The clear side lobes were not observed due to this waveform of emitted wave in this experiments.

Figure 10(b) shows the waveform measured from echo signal from curvature surface of Standard Test Block STB-A1 (ISO 2400). The reflection surface has 100R curvature. The waveform from echo signal is quiet different with the waveform measured by visualization as shown in Fig.10(a). This difference illustrates the importance of visualization analysis for better understanding the sound pressure field made by the ultrasonic wave pulses.

From the comparison of defect directivity analysis, theoretical directivity agreed well with the experimental results in the range of $d/\lambda>1.5$. In the case of angle probe analysis, the range of d/λ was from 2.92 to 5.88 and then, theoretical directivity prediction is expected to agree with the experiments. Theses results suggest that the continuous wave theory can be applied to the range of $d/\lambda>1.5$.

CONCLUSIONS

This paper studied the directivity of ultrasonic wave emitted from the angle probes and reflected from the defects by visualization method. The experimental results were compared with the analysis of continuous wave theory and examined the theory applicability.

Following conclusions were obtained;

1) The directivity of the angle probe agreed well with the theory in terms of the principal lobe. Side lobes were not observed.
2) The sharp directivity existed in the smaller slits compared with the ultrasonic wavelength.
3) The same directivities were obtained, when the parameter d/λ were the same in the case of defect directivity.
4) In the range of $d/\lambda>1.5$, directivity of angle probes and surface defect measured from the visualization agreed with the theoretical directivity.

REFERENCES

1. H.Wustenberg, Technischen Universitat, Berlin (1972).
2. H.Wustenberg, Preprint of 7th ICNT, Warszawa (1973), No H-03.
3. R.Werneyer and U.Schlengermann, Materialpruf, 13 (1971) Nr.7 Juli.
4. R.Werneyer and U.Schlengermann, Materialpruf, 13 (1971) Nr.9 Sept..
5. F.V.Ammirato, Materials Evaluation, Jan. (1977)
6. K.Date, Y.Tabata, and H.Shimada, IEEE Ultrasonics Symposium, (1987), p.1093
7. Y.H.Nam, K.Date and H.Takahashi, Int. Symp. of NDT&SSM,FENDT'92, Tokyo, 1992, p.29.
8. K.Kimura, Report for Basis and Theory of Ultrasonic Non-destructive Testing, (Japan Society for the Promotion of Science), (1974), p.107